

SUPPLEMENTARY INFORMATION

for

SAXS Anti-Peaks Reveal the Length-Scales of Dual

Positive/Negative and Polar/Apolar Ordering in

Room-Temperature Ionic Liquids

Hemant K. Kashyap, Jeevapani J. Hettige, Harsha V. R. Annapureddy, and

Claudio J. Margulis*

Department of Chemistry, University of Iowa, Iowa City, Iowa 52242, USA

E-mail: claudio-margulis@uiowa.edu

*To whom correspondence should be addressed

1 Simulation Details

All simulations were performed using the GROMACS^{1,2} molecular dynamics package. We used the Lopes and Padua³ partial charges for cations and anions. Bonded and Lennard-Jones (LJ) energy parameters were taken from the OPLS-AA⁴ force field as suggested by Lopes and Padua.³ However, the torsional energy parameters for CT-CT-CT-CT, CT-CT-CT-HC and HC-CT-CT-HC dihedrals for alkyl carbons and hydrogens were taken from the improved OPLS-AA(2001) parameter set.⁵ Each system was simulated in a simple cubic box consisting of 3000 ion pairs. Proper periodic boundary conditions and the minimum image convention were applied. Following well established protocols,⁶ we equilibrated our systems by initially running them with scaled partial charges at high temperature and raised charges and lowered temperatures to arrive at fully charged and properly equilibrated densities at 295 K and 1 bar. Subsequently, each system was run in the NPT ensemble for at least 3.5 ns at 295 K and 1 bar. The Nose-Hoover^{7,8} thermostat and Parinello-Rahman⁹ barostat were used as heat and pressure baths. The last 1 ns was saved at a frequency of 1 ps for the calculation of liquid structural properties. The Leap-Frog algorithm with a 1 fs time step, as implemented in GROMACS,^{1,2} was used for integrating the equations of motion. Cutoffs for the LJ and real space part of the Coulombic interactions were set to 15 Å. For the electrostatic interactions we used the Particle Mesh Ewald (PME)^{10,11} summation method with an interpolation order of 6 and 0.08 nm of FFT grid spacing. The final simulated bulk densities of [Pyr_{1,n}⁺][NTf₂⁻] liquids for $n = 4, 6, 8$ and 10 were 1.46, 1.39, 1.33 and 1.29 gm/cc, respectively. A few representative radial distribution functions are provided in Figs. S4 and S5.

Theoretically, the total X-ray structure function, $S(q)$, can be calculated from atom-atom radial pair distribution functions using Eq. (1)

$$S(q) = \frac{\rho_o \sum_i \sum_j x_i x_j f_i(q) f_j(q) \int_0^{\infty} 4\pi r^2 [g_{ij}(r) - 1] \frac{\sin(qr)}{qr} dr}{\left[\sum_i x_i f_i(q) \right]^2}. \quad (1)$$

Here, $g_{ij}(r)$ is the radial pair distribution function for atomic species of type i and j . x_i and $f_i(q)$,

respectively, are the mole fraction and X-ray form factor¹² of the i^{th} type of atom. ρ_o is the total number density of the system.

In order to reduce the effect of finite truncation error, in all our Fourier transforms we include a Lorch window function^{13,14} $W(r) = \frac{\sin(2\pi r/L)}{2\pi r/L}$. The effect of this function when the box length L is large as in the current study is minimal but it may be advantageous in the case of smaller simulation boxes.

Experimentally, $S(q)$ is determined from the coherent X-ray intensity, $I_{coh}(q)$, using following relation:¹⁵

$$S(q) = \frac{I_{coh}(q) - \sum_i x_i f_i^2(q)}{[\sum_i x_i f_i(q)]^2}. \quad (2)$$

Partitioning of $S(q)$ into cationic, anionic and their cross correlations such that $S(q) = S^{c-c}(q) + S^{c-a}(q) + S^{a-c}(q) + S^{a-a}(q)$ leads to the following definitions of subcomponents:¹⁶

$$S^{c-c}(q) = \frac{\rho_o \sum_i \sum_j x_i x_j f_i(q) f_j(q)}{[\sum_i x_i f_i(q)]^2} \int_0^\infty 4\pi r^2 \left[g_{ij}^{c-c}(r) - \lim_{r \rightarrow \infty} g_{ij}^{c-c}(r) \right] \frac{\sin(qr)}{qr} dr$$

$$S^{a-a}(q) = \frac{\rho_o \sum_i \sum_j x_i x_j f_i(q) f_j(q)}{[\sum_i x_i f_i(q)]^2} \int_0^\infty 4\pi r^2 \left[g_{ij}^{a-a}(r) - \lim_{r \rightarrow \infty} g_{ij}^{a-a}(r) \right] \frac{\sin(qr)}{qr} dr \quad (3)$$

and

$$S^{c-a}(q) + S^{a-c}(q) = \frac{\rho_o \sum_i \sum_j x_i x_j f_i(q) f_j(q)}{[\sum_i x_i f_i(q)]^2} \left\{ \begin{array}{l} \int_0^\infty 4\pi r^2 \left[g_{ij}^{c-a}(r) - \lim_{r \rightarrow \infty} g_{ij}^{c-a}(r) \right] \frac{\sin(qr)}{qr} dr \\ + \int_0^\infty 4\pi r^2 \left[g_{ij}^{a-c}(r) - \lim_{r \rightarrow \infty} g_{ij}^{a-c}(r) \right] \frac{\sin(qr)}{qr} dr \end{array} \right\} \quad (4)$$

Here, $g_{ij}^{c-a}(r)$ is the radial distribution function for the i^{th} type of atom in the cation and the j^{th}

type of atom in the anion and are given by,¹⁶

$$\begin{aligned}
 g_{ij}^{c-c}(r) &= \frac{V}{N_i N_j} \sum_i^{N_i^c} \sum_j^{N_j^c} \frac{\delta(r_{ij} - r)}{\frac{4}{3}\pi((r+dr)^3 - r^3)}, \\
 g_{ij}^{c-a}(r) &= \frac{V}{N_i N_j} \sum_i^{N_i^c} \sum_j^{N_j^a} \frac{\delta(r_{ij} - r)}{\frac{4}{3}\pi((r+dr)^3 - r^3)}, \\
 g_{ij}^{a-c}(r) &= \frac{V}{N_i N_j} \sum_i^{N_i^a} \sum_j^{N_j^c} \frac{\delta(r_{ij} - r)}{\frac{4}{3}\pi((r+dr)^3 - r^3)}, \\
 g_{ij}^{a-a}(r) &= \frac{V}{N_i N_j} \sum_i^{N_i^a} \sum_j^{N_j^a} \frac{\delta(r_{ij} - r)}{\frac{4}{3}\pi((r+dr)^3 - r^3)},
 \end{aligned} \tag{5}$$

where V is the volume, N_i is the total number of atoms of type i in the system, and N_i^c , N_i^a are the number of atoms of type i in cations and anions, respectively.

One can further split the cation-cation partial structure function such that $S^{c-c}(q) = S^{cHead-cHead}(q) + S^{cHead-cTail}(q) + S^{cTail-cHead}(q) + S^{cTail-cTail}(q)$ as:

$$\begin{aligned}
 S^{cHead-cHead}(q) &= \frac{\rho_o \sum_i \sum_j x_i x_j f_i(q) f_j(q)}{\left[\sum_i x_i f_i(q) \right]^2} \int_0^\infty 4\pi r^2 \left[g_{ij}^{cHead-cHead}(r) - \lim_{r \rightarrow \infty} g_{ij}^{cHead-cHead}(r) \right] \frac{\sin(qr)}{qr} dr \\
 S^{cTail-cTail}(q) &= \frac{\rho_o \sum_i \sum_j x_i x_j f_i(q) f_j(q)}{\left[\sum_i x_i f_i(q) \right]^2} \int_0^\infty 4\pi r^2 \left[g_{ij}^{cTail-cTail}(r) - \lim_{r \rightarrow \infty} g_{ij}^{cTail-cTail}(r) \right] \frac{\sin(qr)}{qr} dr \tag{6}
 \end{aligned}$$

and

$$S^{cHead-cTail}(q) + S^{cTail-cHead}(q) = \frac{\rho_o \sum_i \sum_j x_i x_j f_i(q) f_j(q)}{\left[\sum_i x_i f_i(q) \right]^2} \left\{ \begin{aligned} &\int_0^\infty 4\pi r^2 \left[g_{ij}^{cHead-cTail}(r) - \lim_{r \rightarrow \infty} g_{ij}^{cHead-cTail}(r) \right] \frac{\sin(qr)}{qr} dr \\ &+ \int_0^\infty 4\pi r^2 \left[g_{ij}^{cTail-cHead}(r) - \lim_{r \rightarrow \infty} g_{ij}^{cTail-cHead}(r) \right] \frac{\sin(qr)}{qr} dr \end{aligned} \right\} \tag{7}$$

In the above equations $g_{ij}^{cHead-cHead}(r)$, $g_{ij}^{cTail-cTail}(r)$, $g_{ij}^{cHead-cTail}(r)$ and $g_{ij}^{cTail-cHead}(r)$ are given

by,

$$\begin{aligned}
 g_{ij}^{cHead-cHead}(r) &= \frac{V}{N_i N_j} \sum_i^{N_i^{cHead}} \sum_j^{N_j^{cHead}} \frac{\delta(r_{ij} - r)}{\frac{4}{3}\pi((r+dr)^3 - r^3)}, \\
 g_{ij}^{cTail-cTail}(r) &= \frac{V}{N_i N_j} \sum_i^{N_i^{cTail}} \sum_j^{N_j^{cTail}} \frac{\delta(r_{ij} - r)}{\frac{4}{3}\pi((r+dr)^3 - r^3)}, \\
 g_{ij}^{cHead-cTail}(r) &= \frac{V}{N_i N_j} \sum_i^{N_i^{cHead}} \sum_j^{N_j^{cTail}} \frac{\delta(r_{ij} - r)}{\frac{4}{3}\pi((r+dr)^3 - r^3)}, \\
 g_{ij}^{cTail-cHead}(r) &= \frac{V}{N_i N_j} \sum_i^{N_i^{cTail}} \sum_j^{N_j^{cHead}} \frac{\delta(r_{ij} - r)}{\frac{4}{3}\pi((r+dr)^3 - r^3)}. \tag{8}
 \end{aligned}$$

In Eqns. (S8), N_i^{cHead} , N_i^{cTail} are the total number of atoms of type i in the polar head and apolar tail of the cation respectively. In this study, we follow the Lopes and Padua charge definitions which imply that the charged part of the cation extends not only to the ring but also to the methyl group and up to the second CH₂ of the longer alkyl tail.³ Therefore our definition of polar head includes these groups and the ring.

Similarly one can split the cation-anion partial structure function so that $[S^{c-a}(q) + S^{a-c}(q)] = S^{cHead-a}(q) + S^{a-cHead}(q) + S^{cTail-a}(q) + S^{a-cTail}(q)$ as:

$$\begin{aligned}
 S^{cHead-a}(q) + S^{a-cHead}(q) &= \frac{\rho_o \sum_i \sum_j x_i x_j f_i(q) f_j(q)}{\left[\sum_i x_i f_i(q) \right]^2} \left\{ \begin{aligned} &\int_0^\infty 4\pi r^2 \left[g_{ij}^{cHead-a}(r) - \lim_{r \rightarrow \infty} g_{ij}^{cHead-a}(r) \right] \frac{\sin(qr)}{qr} dr \\ &+ \int_0^\infty 4\pi r^2 \left[g_{ij}^{a-cHead}(r) - \lim_{r \rightarrow \infty} g_{ij}^{a-cHead}(r) \right] \frac{\sin(qr)}{qr} dr \end{aligned} \right\} \\
 S^{cTail-a}(q) + S^{a-cTail}(q) &= \frac{\rho_o \sum_i \sum_j x_i x_j f_i(q) f_j(q)}{\left[\sum_i x_i f_i(q) \right]^2} \left\{ \begin{aligned} &\int_0^\infty 4\pi r^2 \left[g_{ij}^{cTail-a}(r) - \lim_{r \rightarrow \infty} g_{ij}^{cTail-a}(r) \right] \frac{\sin(qr)}{qr} dr \\ &+ \int_0^\infty 4\pi r^2 \left[g_{ij}^{a-cTail}(r) - \lim_{r \rightarrow \infty} g_{ij}^{a-cTail}(r) \right] \frac{\sin(qr)}{qr} dr \end{aligned} \right\} \tag{9}
 \end{aligned}$$

Here, $g_{ij}^{cHead-a}(r)$, $g_{ij}^{cTail-a}(r)$, $g_{ij}^{a-cHead}(r)$ and $g_{ij}^{a-cTail}(r)$ are given by,

$$\begin{aligned}g_{ij}^{cHead-a}(r) &= \frac{V}{N_i N_j} \sum_i^{N_i^{cHead}} \sum_j^{N_j^a} \frac{\delta(r_{ij} - r)}{\frac{4}{3}\pi((r+dr)^3 - r^3)}, \\g_{ij}^{cTail-a}(r) &= \frac{V}{N_i N_j} \sum_i^{N_i^{cTail}} \sum_j^{N_j^a} \frac{\delta(r_{ij} - r)}{\frac{4}{3}\pi((r+dr)^3 - r^3)}, \\g_{ij}^{a-cHead}(r) &= \frac{V}{N_i N_j} \sum_i^{N_i^a} \sum_j^{N_j^{cHead}} \frac{\delta(r_{ij} - r)}{\frac{4}{3}\pi((r+dr)^3 - r^3)}, \\g_{ij}^{a-cTail}(r) &= \frac{V}{N_i N_j} \sum_i^{N_i^a} \sum_j^{N_j^{cTail}} \frac{\delta(r_{ij} - r)}{\frac{4}{3}\pi((r+dr)^3 - r^3)}.\end{aligned}\tag{10}$$

References

- [1] Hess, B.; Kutzner, C.; van der Spoel, D.; Lindahl, E. *J. Chem. Theory Comput.* **2008**, *4*, 435–447.
- [2] van der Spoel, D.; Lindahl, E.; Hess, B.; Groenhof, G.; Mark, A. E.; Berendsen, H. J. C. *J. Comput. Chem.* **2005**, *26*, 1701–1718.
- [3] Lopes, J. N. C.; Pádua, A. A. H. *J. Phys. Chem. B* **2004**, *108*, 16893–16898.
- [4] Rizzo, R. C.; Jorgensen, W. L. *J. Am. Chem. Soc.* **1999**, *121*, 4827–4836.
- [5] Price, M. L. P.; Ostrovsky, D.; Jorgensen, W. L. *J. Comp. Chem.* **2001**, *22*, 1340–1352.
- [6] Annapureddy, H. V. R.; Kashyap, H. K.; De Biase, P. M.; Margulis, C. J. *J. Phys. Chem. B* **2010**, *114*, 16838–16846.
- [7] Nose, S. *J. Chem. Phys.* **1984**, *81*, 511–519.
- [8] Nose, S. *Mol. Phys.* **1984**, *52*, 255 – 268.
- [9] Parrinello, M.; Rahman, A. *J. Appl. Phys.* **1981**, *52*, 7182–7190.
- [10] Darden, T.; York, D.; Pedersen, L. *J. Chem. Phys.* **1993**, *98*, 10089–10092.

- [11] Essmann, U.; Perera, L.; Berkowitz, M. L.; Darden, T.; Lee, H.; Pedersen, L. G. *J. Chem. Phys.* **1995**, *103*, 8577–8593.
- [12] Prince, E., Ed. *International Tables for Crystallography*; International Union of Crystallography, 2006; Vol. C.
- [13] Lorch, E. *J. Phys. C: Solid State Phys.* **1969**, *2*, 229–237.
- [14] Du, J.; Benmore, C. J.; Corrales, R.; Hart, R. T.; Weber, J. K. R. *Journal of Physics: Condensed Matter* **2009**, *21*, 205102.
- [15] Keen, D. A. *J. Appl. Cryst.* **2001**, *34*, 172–177.
- [16] Santos, C. S.; Annapureddy, H. V. R.; Murthy, N. S.; Kashyap, H. K.; Castner, Jr., E. W.; Margulis, C. J. *J. Chem. Phys.* **2011**, *134*, 064501.

2 Supporting Figures

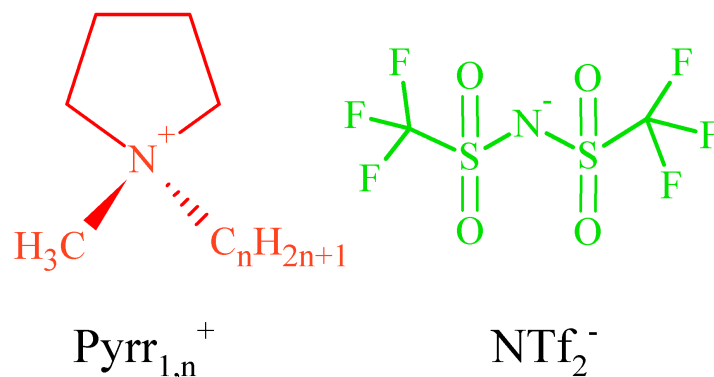


Figure 1: Chemical Structure of 1-alkyl-1-methylpyrrolidinium cation (left) and bis(trifluoromethylsulfonyl)amide anion (right).

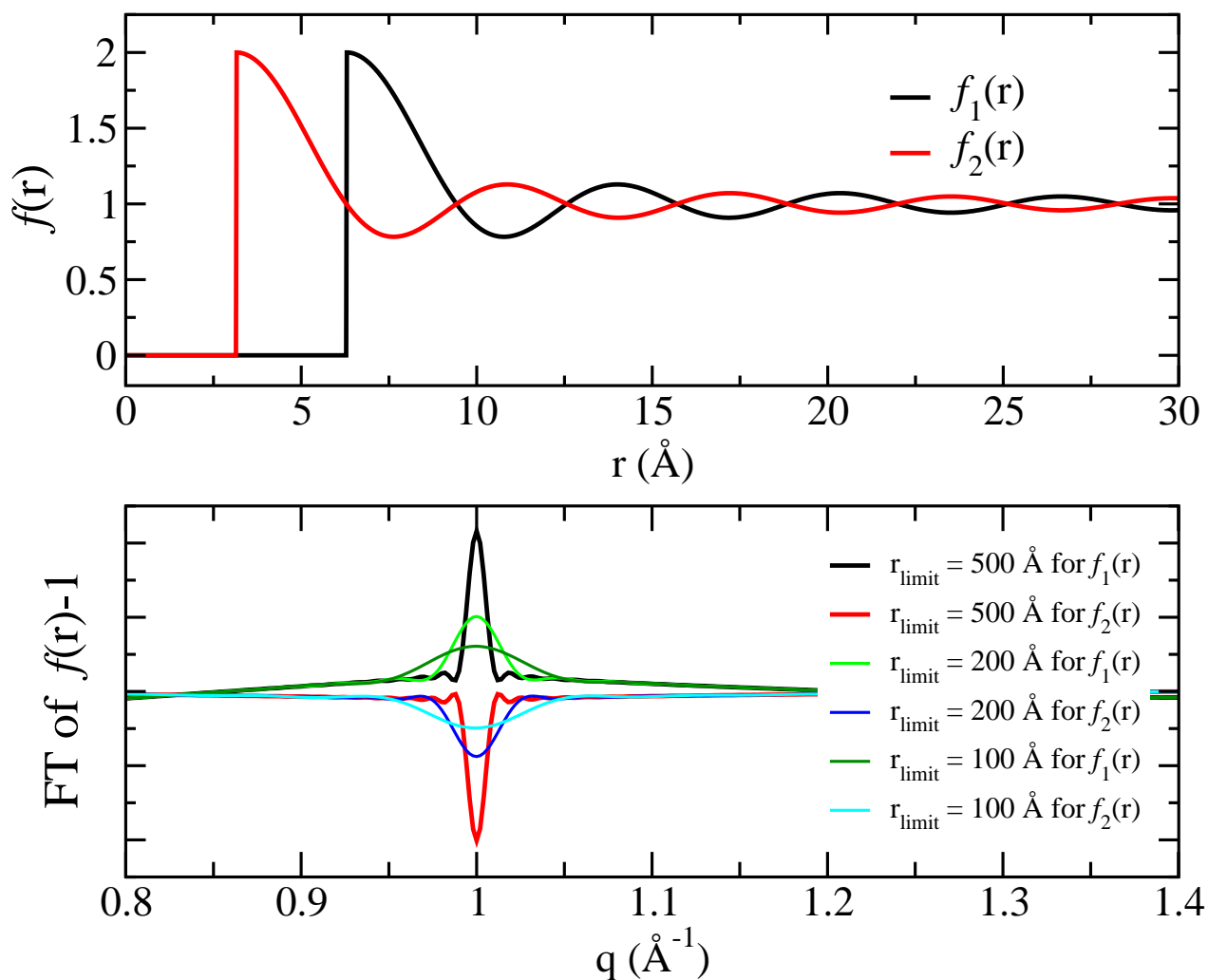


Figure 2: *Top*: Idealized single spatial periodicity rdf functions $f(r)$ defined as $1 + \sin(k(r - r_0))/(k(r - r_0))$ for $r > r_0$ and zero otherwise. In all cases, $k = 1 \text{ Å}^{-1}$. r_0 is set to $2\pi/k$ and π/k for $f_1(r)$ and $f_2(r)$, respectively. *Bottom*: The 3D Fourier transforms (FT) of $f(r)$ corresponding to an idealized single wavenumber SAXS $S(q)$. Since $f(r)$ is infinitely periodic the FT is a function of the upper integration limit, r_{limit} . In the case of liquids, $g(r)$ loses correlations after a few oscillations and therefore peaks in $S(q)$ appear to be broad. This figure shows that $f(r)$ functions of the same spatial periodicity but with a π spatial phase offset result in peaks and anti-peaks in reciprocal space.

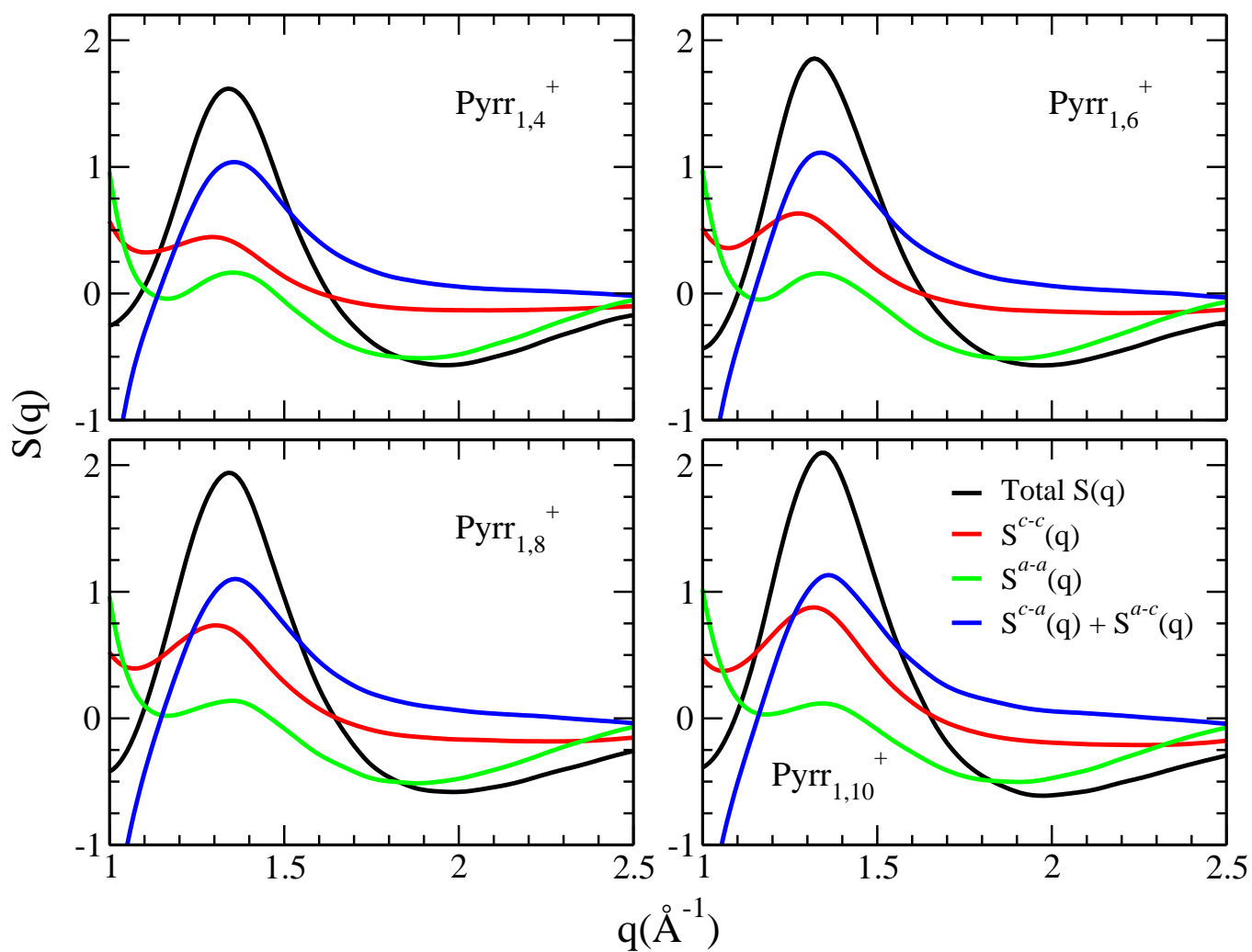


Figure 3: Total $S(q)$ (*black*), cation-cation (*red*), anion-anion (*green*) and cation-anion (*blue*) partial structure functions magnified at the location of the most intense q peak below 2\AA^{-1} . From this figure we can gauge the relative cation-anion and cation-cation contributions to the adjacency peak.

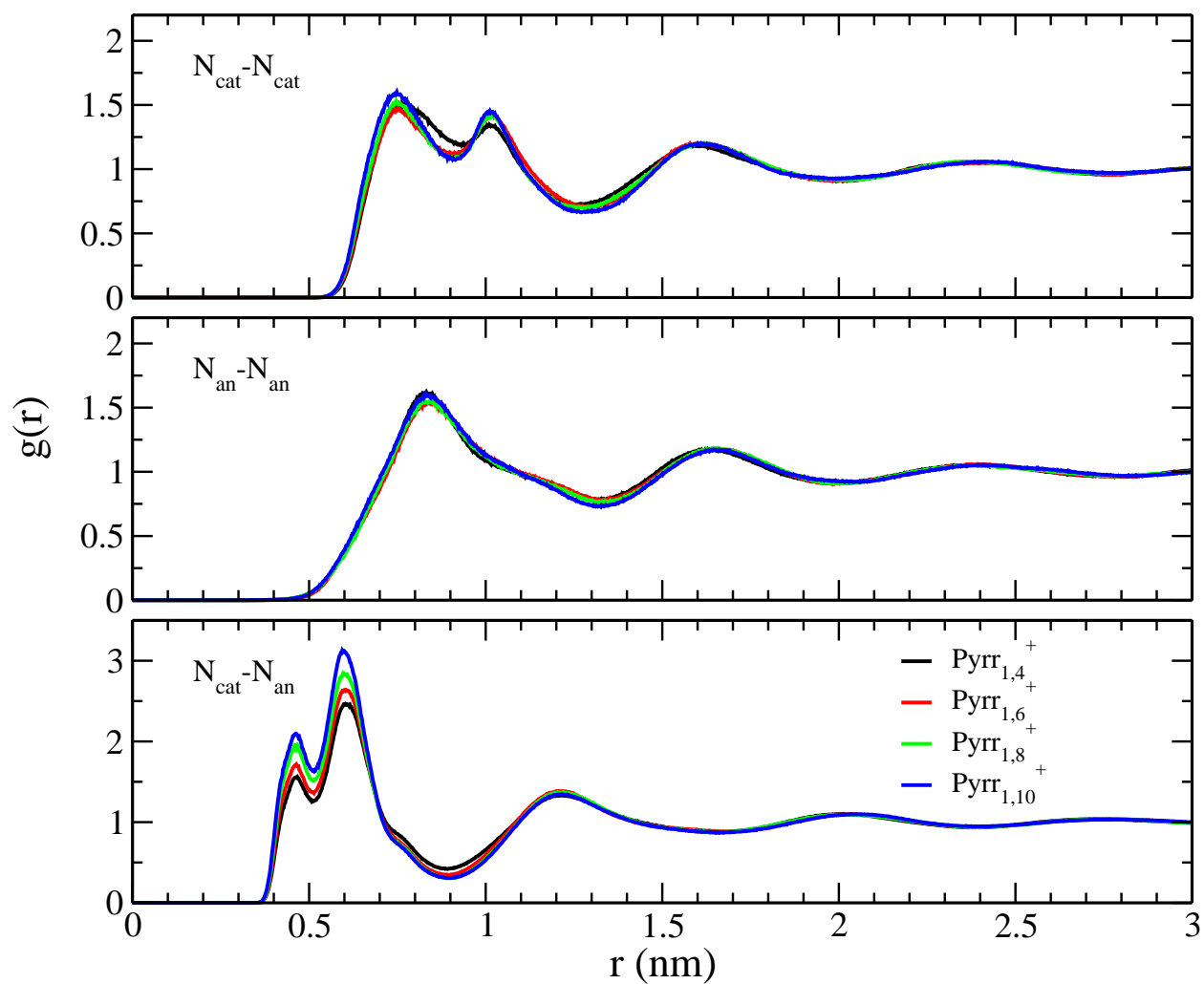


Figure 4: Radial distribution functions for cation nitrogen (top pannel), anion nitrogen (middle panel) and cation and anion nitrogen (bottom panel). It is clear from the $N_{cat}-N_{an}$ rdfs that correlations between charged groups become stronger when the cationic chain length is increased.

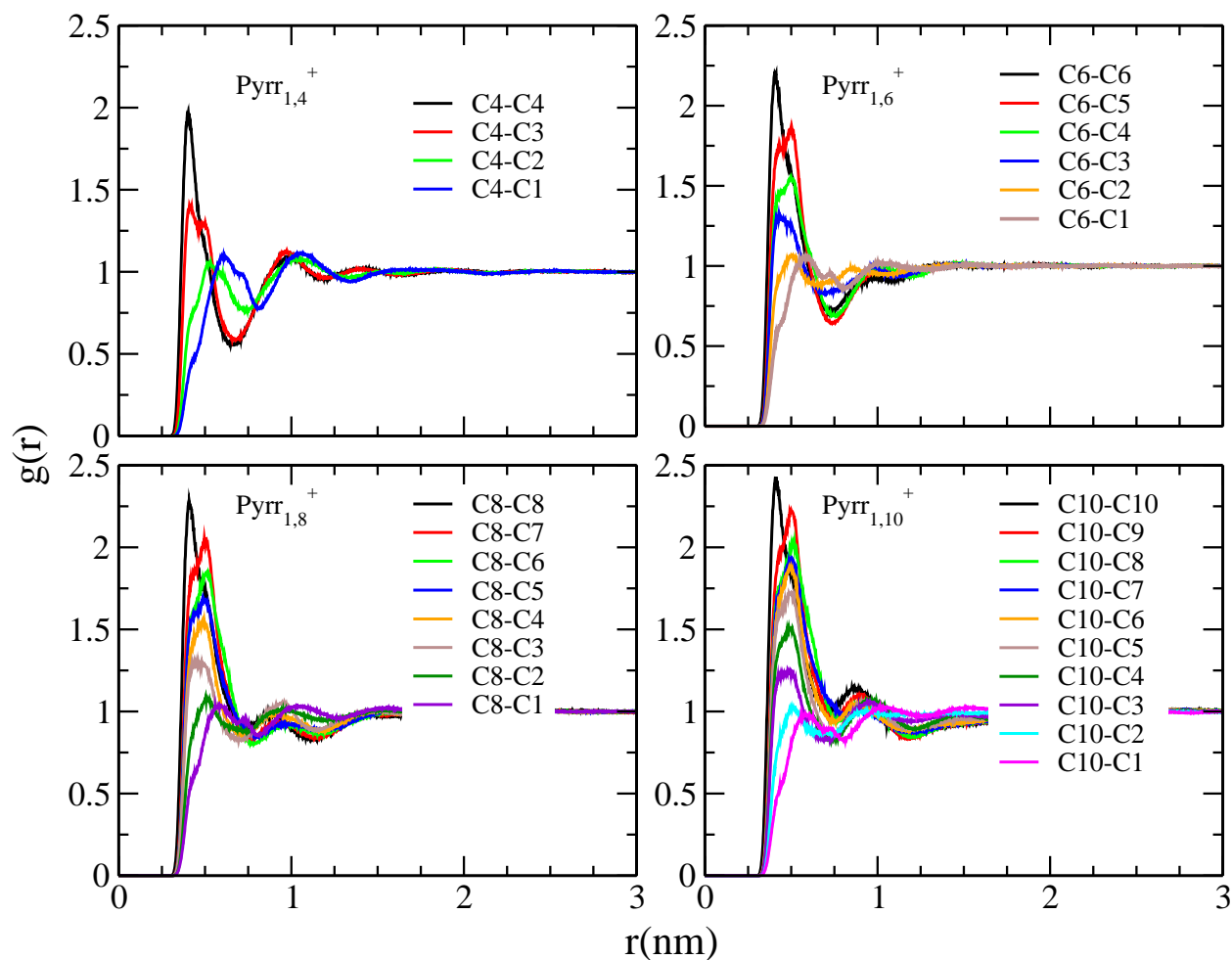


Figure 5: Radial distribution functions for carbon atoms in the alkyl tail of the pyrrolidinium cations. Numbering is set to C1 for the carbon atom adjacent to the ring N. Clearly, in the case of cations with longer alkyl tails the stronger N_{cat} - N_{an} correlations in Fig. S4 are accompanied by enhanced apolar-apolar correlations.